

# Further explorations of Skyrme-Hartree-Fock-Bogoliubov mass formulas. XI: Stabilizing neutron stars against a ferromagnetic collapse.

N. Chamel,<sup>1</sup> S. Goriely,<sup>1</sup> and J. M. Pearson<sup>2</sup>

<sup>1</sup>*Institut d'Astronomie et d'Astrophysique, CP-226,  
Université Libre de Bruxelles, 1050 Brussels, Belgium*

<sup>2</sup>*Dépt. de Physique, Université de Montréal,  
Montréal (Québec), H3C 3J7 Canada*

(Dated: November 3, 2018)

## Abstract

We construct a new Hartree-Fock-Bogoliubov (HFB) mass model, labeled HFB-18, with a generalized Skyrme force. The additional terms that we have introduced into the force are density-dependent generalizations of the usual  $t_1$  and  $t_2$  terms, and are chosen in such a way as to avoid the high-density ferromagnetic instability of neutron stars that is a general feature of conventional Skyrme forces, and in particular of the Skyrme forces underlying all the HFB mass models that we have developed in the past. The remaining parameters of the model are then fitted to essentially all the available mass data, an rms deviation  $\sigma$  of 0.585 MeV being obtained. The new model thus gives almost as good a mass fit as our best-fit model HFB-17 ( $\sigma = 0.581$  MeV), and has the advantage of avoiding the ferromagnetic collapse of neutron stars.

PACS numbers: 21.10.Dr, 21.30.-x, 21.60.Jz, 26.60.Dd, 26.60.Kp

## I. INTRODUCTION

Astrophysical considerations require that one have available nuclear-mass models as rigorously based as possible. In this way one might hope to be able to extrapolate from the mass data, which cluster fairly closely to the stability line, out towards the neutron drip line, and make reliable estimates of the masses of nuclei so neutron rich that there is no hope of measuring them in the foreseeable future; such nuclei are found in the outer crusts of neutron stars, and also play a vital role in the r-process of nucleosynthesis. To this end we have developed a series of nuclear-mass models based on the Hartree-Fock-Bogoliubov (HFB) method with Skyrme and contact-pairing forces, together with phenomenological Wigner terms and correction terms for the spurious collective energy; all the model parameters are fitted to essentially all the experimental mass data (see Ref. [1] and references quoted therein). To make the extrapolations to neutron-rich nuclei as reliable as possible, the underlying Skyrme force in model HFB-9 [2] and all later models was constrained to fit the zero-temperature equation of state (EoS) of neutron matter (NeuM), as calculated by Friedman and Pandharipande [3] (FP) for realistic two- and three-nucleon forces. (We have so far been unable to obtain mass fits as good as our published ones when constraining to the more complete, and slightly stiffer, realistic neutron-matter EoS labeled A18 +  $\delta v$  + UIX\* [4]. Our findings are consistent with a recent analysis of the  $\pi^-/\pi^+$  ratio in central heavy-ion collisions indicating that this EoS is too stiff [5].)

Because of the neutron-matter constraint our models can be used to extrapolate beyond the neutron drip line and calculate with some confidence the EoS of the inner crust of neutron stars [6] (throughout this paper we assume zero temperature). Since the good agreement of our forces with the FP calculation [3] of neutron matter extends to the highest density encountered in neutron stars it might be thought that our inner-crust EoS is continuous with that of the homogeneous core, the transition between the two regions taking place at around  $0.5\rho_0$ , where  $\rho_0$  ( $\simeq 0.16$  nucleons.fm $^{-3}$ ) is the equilibrium density of symmetric nuclear matter (SNM). However, in fitting our forces to the neutron matter of FP [3], we *assume* that our ground state is spin unpolarized, but in fact the underlying Skyrme forces of all our models, like all conventional Skyrme forces of the form (1), predict that beyond a certain supernuclear density the ground state of NeuM becomes ferromagnetic, i.e., at least partially polarized [7, 8, 9]. In the case of the Skyrme force BSk17, the force underlying our best-fit

model, HFB-17 [1], complete polarization sets in at a density of  $\rho_{frm} = 1.24 \rho_0$ . On the other hand, microscopic calculations using different realistic forces and different methods [10, 11, 12, 13, 14] all predict no such polarization, at least up to about  $5\rho_0$ . Moreover, in the case of all our own previously published HFB forces the predicted ferromagnetic state is unstable against collapse, the energy becoming more and more negative as the density increases (see, for example, the lowest curve in Fig. 1, constructed for force BSk17). This predicted ferromagnetic collapse sets in at densities that are certainly encountered in the cores of all neutron stars, and is contradicted by the very existence of neutron stars.

Actually, the core of neutron stars does not consist of pure NeuM but rather of so-called neutron-star matter (N\*M), which just below the crust is composed of neutrons with a weak admixture of proton-electron pairs in beta equilibrium (for simplicity we will assume that these are the only particles present also at higher densities). But if NeuM were indeed unstable against collapse then N\*M would be likewise, since, at the very least, it would always be energetically advantageous for N\*M to spontaneously transform into NeuM through electron capture beyond some critical density. Thus the stability of NeuM against collapse is a necessary condition for the existence of neutron stars. But even if no such instability is implied, there is a general tendency for Skyrme forces of the conventional form (1) to lead to the ground state of N\*M being polarized. However, calculations based on realistic forces show the ground state of N\*M, like that of NeuM, to be unpolarized at all densities [15].

Our purpose here is to show that by adding suitable terms to the Skyrme force it is possible to eliminate the anomalous prediction of a ferromagnetic transition in neutron stars, with essentially no impact on the high-quality fits to the mass data that we have previously obtained with conventional Skyrme forces. (An alternative approach to this problem has been followed by Margueron *et al.* [16, 17].) In Section II we discuss in more detail the nature of the spurious transition to a ferromagnetic state in NeuM and N\*M associated with conventional Skyrme forces of the form (1), considering not only our own BSk17 [1], but also the widely used SLy4 [18], which was specifically constructed for neutron-star calculations. Section III shows how extra terms in the Skyrme force can stop this spurious transition, while in Section IV we describe the new mass fit. Our conclusions are summarized in Section V, and in the Appendix we present the full formalism for the generalized form of Skyrme force used here.

## II. FERROMAGNETIC INSTABILITY

The Skyrme forces that we have used in all our previously published HFB models have the conventional form

$$\begin{aligned}
v_{i,j} = & t_0(1 + x_0 P_\sigma) \delta(\mathbf{r}_{ij}) + \frac{1}{2} t_1 (1 + x_1 P_\sigma) \frac{1}{\hbar^2} [p_{ij}^2 \delta(\mathbf{r}_{ij}) + \delta(\mathbf{r}_{ij}) p_{ij}^2] \\
& + t_2 (1 + x_2 P_\sigma) \frac{1}{\hbar^2} \mathbf{p}_{ij} \cdot \delta(\mathbf{r}_{ij}) \mathbf{p}_{ij} + \frac{1}{6} t_3 (1 + x_3 P_\sigma) \rho(\mathbf{r})^\alpha \delta(\mathbf{r}_{ij}) \\
& + \frac{i}{\hbar^2} W_0 (\boldsymbol{\sigma}_i + \boldsymbol{\sigma}_j) \cdot \mathbf{p}_{ij} \times \delta(\mathbf{r}_{ij}) \mathbf{p}_{ij} \quad , \tag{1}
\end{aligned}$$

where  $\mathbf{r}_{ij} = \mathbf{r}_i - \mathbf{r}_j$ ,  $\mathbf{r} = (\mathbf{r}_i + \mathbf{r}_j)/2$ ,  $\mathbf{p}_{ij} = -i\hbar(\nabla_i - \nabla_j)/2$  is the relative momentum,  $P_\sigma$  is the two-body spin-exchange operator, and  $\rho(\mathbf{r}) = \rho_n(\mathbf{r}) + \rho_p(\mathbf{r})$  is the total local density,  $\rho_n(\mathbf{r})$  and  $\rho_p(\mathbf{r})$  being the neutron and proton densities, respectively.

The fit of the parameters of this form of force to the nuclear masses, and the various other constraints mentioned above, leave us absolutely no freedom to avoid an unphysical ferromagnetic collapse of NeuM. The situation for our force BSk17 is shown in Figs. 1 and 2. (The corresponding curves for force SLy4 [18] shown in these two figures are discussed below.) These curves have been calculated using Eq. (C. 14) of Bender *et al.* [19], which gives the energy per nucleon of homogeneous nuclear matter with arbitrary charge asymmetry and degree of polarization; we define the latter quantity for nucleons of charge type  $q$  ( $q = n$  or  $p$ ) by

$$I_{\sigma q} = \frac{\rho_{q\uparrow} - \rho_{q\downarrow}}{\rho_{q\uparrow} + \rho_{q\downarrow}} \quad . \tag{2}$$

The curve labeled ‘‘BSk17: no polarization’’ in Fig. 1 shows the energy per neutron calculated under the constraint  $I_{\sigma n} = 0$ , while the curve ‘‘BSk17: polarization allowed’’ shows the same quantity calculated at each density by minimizing the energy per neutron with respect to  $I_{\sigma n}$ . The first of these curves is seen to be in excellent agreement with the realistic EoS of NeuM given by FP [3], but the second curve shows that this agreement is destroyed when polarization is allowed, the system collapsing. The corresponding value of  $I_{\sigma n}$  for BSk17 is shown in Fig. 2; the rapidity with which polarization sets in with increasing density will be seen.

As for N\*M, to the nuclear energy corresponding to the Skyrme force in this neutron-proton mixture we have to add the electron kinetic energy, for the density of which we take

the exact expression (see, for example, Section 24.6c of Ref. [20])

$$u_e = \frac{mc^2}{24\pi^2} \left(\frac{mc}{\hbar}\right)^3 \{-8x^3 + 3x(1+2x^2)(1+x^2)^{1/2} - 3\sinh^{-1}x\}, \quad (3)$$

where

$$x = \frac{\hbar}{mc} (3\pi^2\rho_e)^{1/3}, \quad (4)$$

$\rho_e$  being the electron density (equal to the proton density  $\rho_p$ , because of electric-charge neutrality). We minimize the total energy per nucleon with respect to the proton fraction  $Y_e = \rho_p/\rho$ , while imposing the constraint  $I_{\sigma n} = I_{\sigma p} = 0$ , and obtain the curve labeled “BSk17: no polarization” in Fig. 3. If we next minimize the total energy with respect to  $Y_e, I_{\sigma n}$  and  $I_{\sigma p}$  we obtain the curve labeled “BSk17: polarization allowed” in Fig. 3; the corresponding values of  $Y_e, I_{\sigma n}$  and  $I_{\sigma p}$  as a function of density are shown in Fig. 4. It will be seen that once polarization is admitted BSk17 leads in N\*M to the same instability with respect to collapse that we found in NeuM (Fig. 1).

*The case of Skyrme force SLy4.* Figs. 1 and 3 also show the corresponding curves for force SLy4 [18] in NeuM and N\*M, respectively. It will be seen that in NeuM (Fig. 1), the onset of polarization has been postponed to  $\rho_{fmg} = 4.4\rho_0$ , and that although there is a considerable softening of the EoS there is no collapse, at least at neutron-star densities. However, Fig. 3 shows that although there is still no collapse in N\*M, the transition to a spurious ferromagnetic state, and the associated softening of the EoS, takes place at the much lower density of  $\rho_{fmg} = 2.5\rho_0$ , which certainly lies within the range of densities found in neutron stars. This shows that stability against a ferromagnetic transition in NeuM at a given density does not guarantee stability in N\*M at the same density. (A similar conclusion has been reached in Ref. [16].)

The fact that SLy4 has greater stability against polarization than does BSk17 is a result of setting  $x_2 = -1$ . Now within the framework of a conventional Skyrme force of the form (1) we have been unable to find an acceptable mass fit for  $x_2 = -1$ , and indeed SLy4 performs badly as a global mass model, the rms deviation for the even-even nuclei being quoted as 5.1 MeV [21]. This could have implications for the composition of both the outer and inner crusts, and might explain the differences between SLy4 and BSk14 predictions shown in Figures 1 and 2 of Ref.[6]. It seems that it is impossible to have both a good mass fit and stability against polarization with the conventional form (1) of Skyrme force.

### III. STABILITY RESTORED

We note now that the form (1) does not exhaust the possibilities for a Skyrme-type force, and we shall consider here two extra terms, writing our complete Skyrme force as

$$v'_{i,j} = v_{i,j} + \frac{1}{2}t_4(1 + x_4P_\sigma)\frac{1}{\hbar^2} \{p_{ij}^2 \rho(\mathbf{r})^\beta \delta(\mathbf{r}_{ij}) + \delta(\mathbf{r}_{ij}) \rho(\mathbf{r})^\beta p_{ij}^2\} \\ + t_5(1 + x_5P_\sigma)\frac{1}{\hbar^2}\mathbf{p}_{ij}\cdot\rho(\mathbf{r})^\gamma \delta(\mathbf{r}_{ij})\mathbf{p}_{ij} \quad . \quad (5)$$

The  $t_4$  and  $t_5$  terms are density-dependent generalizations of the  $t_1$  and  $t_2$  terms, respectively. The formalism for this generalized Skyrme force is developed in Appendix A, where we show in particular that Eq. (C. 14) of Bender *et al.* [19] for homogeneous nuclear matter of arbitrary charge asymmetry and polarization can be generalized to include the new terms simply by making the substitutions of Eqs. (A31a) - (A31d).

We consider now just the simpler case of NeuM, the stabilization of which is a necessary condition. For complete polarization in the presence of the conventional Skyrme force (1) the energy per nucleon is given by [8]

$$e = \frac{3\hbar^2}{10M_n}(6\pi^2\rho)^{2/3} + \frac{3}{10}(6\pi^2)^{2/3}t_2(1 + x_2)\rho^{5/3} \quad . \quad (6)$$

The only Skyrme term operative here is the one in  $t_2$ . The ferromagnetic collapse of neutron matter predicted by all our Skyrme forces at supernuclear densities arises from the fact that the combination  $t_2(1 + x_2)$  is always negative. However, stability can always be enforced by adding a new repulsive term in  $t_5$ , as can be seen from Eqs. (A31c) and (A31d). But we do not want to disturb in any way the unpolarized configuration of NeuM, since we know from the experience with our recent mass models that with the conventional form of Skyrme force (1) alone it is easy to fit the realistic EoS of FP [3], and wish to do so here with the new model. As the energy per nucleon of this latter configuration in the presence of the conventional Skyrme force (1) is given by

$$e = \frac{3\hbar^2}{10M_n}(3\pi^2\rho)^{2/3} + \frac{1}{4}t_0(1 - x_0)\rho + \frac{1}{24}t_3(1 - x_3)\rho^{\alpha+1} \\ + \frac{3}{40}(3\pi^2)^{2/3} \{t_1(1 - x_1) + 3t_2(1 + x_2)\} \rho^{5/3} \quad (7)$$

(see Eq. (A26)), it follows from Eqs. (A31a) and (A31b) that the  $t_5$  term can be completely canceled in unpolarized NeuM by adding a  $t_4$  term with its parameters constrained by

$$\beta = \gamma \quad (8)$$

and

$$t_4(1 - x_4) = -3t_5(1 + x_5) \quad . \quad (9)$$

It is now highly convenient to require that the stabilizing terms in  $t_4$  and  $t_5$  cancel completely in unpolarized nuclear matter of *any* charge asymmetry. This leads, using Eq. (A13), to a second condition on  $t_4$ ,

$$t_4 = -\frac{1}{3}t_5(5 + 4x_5) \quad , \quad (10)$$

which, combined with Eq. (9), leads to

$$x_4 = -\frac{4 + 5x_5}{5 + 4x_5} \quad . \quad (11)$$

Thus all three parameters of the  $t_4$  term will be completely determined by the parameters of the  $t_5$  term, i.e.,  $t_5$ ,  $x_5$  and  $\gamma$ . These latter three parameters leave us with ample flexibility for stabilizing NeuM against polarization, and possible collapse. We stress, however, that it will also be necessary to check the stability of N\*M.

#### IV. THE HFB-18 MASS MODEL

Even though the new terms exactly cancel in homogeneous nuclear matter they will not do so in finite nuclei, and we cannot simply add them on to the BSk17 force. Rather it will be necessary to make a complete refit of all the model parameters to the mass data.

Our HFB calculations for finite nuclei are performed exactly as for the HFB-17 model [1]. In particular, the treatment of pairing, which is neglected in the neutron-matter constraints discussed in the previous section, is highly realistic. As usual, we take a contact pairing force that acts only between nucleons of the same charge state  $q$ ,

$$v_q^{\text{pair}}(\mathbf{r}_i, \mathbf{r}_j) = v^{\pi q}[\rho_n(\mathbf{r}), \rho_p(\mathbf{r})] \delta(\mathbf{r}_{ij}) \quad , \quad (12)$$

where the strength  $v^{\pi q}[\rho_n, \rho_p]$  is a functional of both the neutron and proton densities. But instead of postulating a simple functional form for the density dependence, as is usually done, we construct the pairing force by solving the HFB equations in uniform asymmetric nuclear matter with the appropriate neutron and proton densities, requiring that the resulting gap reproduce exactly, as a function of density, the microscopic  $^1S_0$  pairing gap

calculated with realistic forces [22]. We follow our usual practice of allowing the proton pairing strength to be different from the neutron pairing strength, and for allowing each of these strengths to depend on whether there is an even or odd number of nucleons of the charge type in question. These extra degrees of freedom are taken into account by multiplying the value of  $v^{\pi q}[\rho_n, \rho_p]$ , as determined by the nuclear-matter calculations that we have just described, with renormalizing factors  $f_q^\pm$ , where  $f_p^+$ ,  $f_p^-$  and  $f_n^-$  are free, density-independent parameters to be included in the mass fit, and we set  $f_n^+ = 1$ .

To the HFB energy calculated for the Skyrme and pairing forces we add a Wigner correction,

$$E_W = V_W \exp \left\{ -\lambda \left( \frac{N-Z}{A} \right)^2 \right\} + V'_W |N-Z| \exp \left\{ -\left( \frac{A}{A_0} \right)^2 \right\} , \quad (13)$$

which contributes significantly only for light nuclei with  $N$  close to  $Z$ . Our treatment of this correction is purely phenomenological, although physical interpretations of each of the two terms can be made [23, 24].

A second correction that must be made is to subtract from the HFB energy an estimate for the spurious collective energy. As described in Ref. [24], the form we adopt here is

$$E_{coll} = E_{rot}^{crank} \left\{ b \tanh(c|\beta_2|) + d|\beta_2| \exp\{-l(|\beta_2| - \beta_2^0)^2\} \right\} , \quad (14)$$

in which  $E_{rot}^{crank}$  denotes the cranking-model value of the rotational correction and  $\beta_2$  the quadrupole deformation, while all other parameters are free fitting parameters.

The final correction that we make is to drop Coulomb exchange. This is a device that we have successfully adopted in our most recent models, beginning with HFB-15 [25], and it can be interpreted as simulating neglected effects such as Coulomb correlations, charge-symmetry breaking of the nuclear forces, and vacuum polarization.

The parameters of the model, i.e., of the Skyrme and pairing forces, and of the Wigner and collective corrections, are fitted to the same set of mass data as are all our models since HFB-9 [2], namely, the 2149 measured masses of nuclei with  $N$  and  $Z \geq 8$  given in the 2003 Atomic Mass Evaluation [26]. This fit is subject to the constraints on both unpolarized and polarized NeuM discussed in the previous section, as well as our usual requirement that the isoscalar effective mass  $M_s^*$  take the realistic value of  $0.8M$  in SNM at the equilibrium density  $\rho_0$ . The values of the Skyrme, pairing and Wigner parameters resulting from this

fit are shown in Table I ( $\varepsilon_\Lambda$  is the pairing cutoff parameter [1, 24]): this defines the BSk18 “force”. The parameters of the collective correction are shown in Table II.

The starting point for the new fit was the force BSk17 [1], and we stress that the parameter search was far from exhaustive, particularly with regards to  $t_5$ ,  $x_5$  and  $\gamma$ . Our choice of these latter parameters was somewhat arbitrary, being limited only by the requirements that the energy-density curve for polarized NeuM lie entirely above that for unpolarized NeuM, and that there be no significant deterioration in the quality of the overall mass fit. That the first of these requirements is satisfied is seen in Fig. 5, which automatically guarantees the stability of NeuM against polarization. Proceeding as in Section II, we have checked also that N\*M is stable against polarization over the same density range, as seen in Figs. 6 and 7 (force BSk17 gives virtually identical results in N\*M, provided we do not allow the ground state to be polarized for this force). Likewise, it is apparent in the first line of Table III that we have satisfied the requirement on the quality of the mass fit, and indeed it can be seen from this table that in some respects the new model is better than the old. The fact that large regions of the extended parameter space remain unexplored allows ample scope for future improvement, both with respect to the quality of the mass fit and conformity of the force to reality. Note, however, that as long as our force is constrained by Eqs. (8), (10) and (11) the  $t_4$  and  $t_5$  components of the force will not contribute to the effective mass, and it will not be possible to exploit the advantages of a surface-peaked effective mass [27]: see Eq. (A10).

The comparison of the new parameter set with the original BSk17 set in Table I shows that the changes in the  $t_1$  and  $t_2$  terms are much greater than those in the  $t_0$  and  $t_3$  terms; this simply reflects the fact that the new  $t_4$  and  $t_5$  terms cancel in homogeneous unpolarized matter, and act only through the gradient terms to which they give rise. (Their contribution to the binding is nevertheless far from negligible, amounting to 38 MeV in the case of  $^{208}\text{Pb}$ .) For the same reason there is very little difference between the BSk17 and BSk18 values of the droplet-model parameters [28] shown in the first five lines of Table IV. There is likewise very little change in most of the Landau parameters shown in the last eight lines of Table IV. Only  $G_0$  and  $G_1$  show any substantial differences between BSk17 and BSk18, these being the only two Landau parameters to which the  $t_4$  and  $t_5$  components can contribute when the condition (8) holds and the particular choice  $t_4 = t_5$  is made. In particular, the generalized Skyrme force BSk18 leads to  $G_0$  being larger than -1 in SNM for all densities, thus removing

the spin instability that was predicted by our previous force BSk17, as can be seen in Figure 9. On the other hand, a spin-isospin instability still occurs in SNM at about the same high density as that found for BSk17, the two forces giving very similar values of  $G'_0$  for all densities (see Figure 10). However, insofar as beta-equilibrated N\*M has, as we have seen, a large neutron excess, this spin-isospin instability in SNM is of no consequence for neutron stars.

Finally, we have checked that with the new interaction, BSk18, causality is satisfied in NeuM for all densities found in neutron stars, i.e, the velocity of sound  $v_s$  is smaller than the velocity of light  $c$ . The former is given by the relativistic expression

$$v_s = c \sqrt{\frac{\partial P(\rho)}{\partial \mathcal{E}(\rho)}} \quad , \quad (15)$$

in which  $P(\rho)$  is the pressure,

$$P(\rho) = \rho^2 \frac{\partial e(\rho)}{\partial \rho} \quad (16)$$

and  $\mathcal{E}(\rho)$  is the total energy density,

$$\mathcal{E}(\rho) = \rho (e(\rho) + M_n c^2) \quad , \quad (17)$$

$e(\rho)$  being simply the energy per neutron, as given by Eq. (A26). The calculated value of  $v_s/c$  for BSk18 is shown as a function of  $\rho$  in Fig. 8.

Using this interaction BSk18, we have constructed a complete mass table, labeled HFB-18, running from one drip line to the other over the range  $Z$  and  $N \geq 8$  and  $Z \leq 110$ . The results are very similar to those for HFB-17, the rms difference between all 8389 predictions being 0.433 MeV, and the mean difference (HFB-18 - HFB-17) 0.198 MeV. We have also calculated the spins and parities of all these nuclei; only for about 10% of these nuclei is there a difference with respect to the HFB-17 prediction.

## V. CONCLUSIONS.

We have extended our earlier Skyrme-HFB mass models by the inclusion of terms that are density-dependent generalizations of the usual  $t_1$  and  $t_2$  terms. We have shown that these new terms can be chosen in such a way as to prevent the high-density ferromagnetic collapse of neutron stars that was a general feature of our previous HFB mass models,

without compromising the excellent fit to the mass data that we obtained in the past, and without relaxing any of the previously imposed constraints of conformity to reality. The mass predictions made by the new model, HFB-18, are, in fact, very similar to those made by the preceding model, HFB-17 [1]. These two models not only give better fits to the mass data than does any other published model except that of Duflo and Zucker [29], but they are also by far the most microscopically founded models, and in particular their underlying interactions (BSk17 and BSk18, respectively) have been fitted to realistic calculations of both the EoS and the  $^1S_0$  gap of neutron matter. They can thus be expected to make more reliable predictions of the highly neutron-rich nuclei that appear in the outer crust of neutron stars and that are involved in the r-process. Moreover, these mass models can be used to extrapolate beyond the drip line to the inner crust of neutron stars, using the respective interactions to calculate the EoS in this region. Our confidence in this extrapolation derives not only from the fit of the interactions to neutron matter but also from the precision fit to masses, which means that the presence of protons and the existence of inhomogeneities in the inner crust are well represented.

Finally, pursuing our aim of a unified treatment of the different regions of a neutron star, we can use these effective interactions to calculate the EoS of the homogeneous core (at least in its outer parts where no complications from the possible appearance of hyperons and other particles arise). Of course, for pure NeuM nothing new can be obtained in this way beyond what has already been given by the realistic calculations to which our effective interactions have been fitted, but these interactions can then be reliably used to calculate N\*M, which is not treated in the realistic calculations of FP [3]. Another important application of these effective interactions, which would hardly be practical with realistic forces, is to make a detailed study of the transition between the inner crust and the fluid core.

We have seen that for N\*M, as for masses, the two interactions BSk17 and BSk18 give very similar results, provided we assume that the ground state for the former is unpolarized, which in fact is not the case. Here lies the basic difference between the two interactions: with BSk18 the ground state of NeuM and N\*M is indeed unpolarized at all densities prevailing in neutron stars. This elimination of the spurious polarization is the essential contribution of this paper, made possible by the introduction of the terms in  $t_4$  and  $t_5$ . However, we have so far made only a partial search in the new, extended parameter space, and there remains the possibility not only of improving the fit to the mass data still further but also

of imposing further realistic constraints on the Skyrme force.

## APPENDIX A: FORMALISM FOR GENERALIZED SKYRME FORCE.

The formalism for the conventional Skyrme force (1), with expressions for the energy density, single-particle fields, etc., has been given many times, and is conveniently summarized in Brack *et al.* [30]. The extension to cover the  $t_4$  terms was given by Farine *et al.* [27], but the  $t_5$  terms have not, to our knowledge, been dealt with before, except for the special case where the exponent  $\gamma$  is set equal to 1 [31].

*Energy density.*

Assuming invariance under time reversal, the HFB energy is written as the integral of a purely local energy-density functional

$$E_{\text{HFB}} = \int \mathcal{E}_{\text{HFB}}(\mathbf{r}) d^3\mathbf{r} \quad , \quad (\text{A1})$$

where

$$\begin{aligned} \mathcal{E}_{\text{HFB}}(\mathbf{r}) = & \mathcal{E}_{\text{Sky}} \left[ \rho_n(\mathbf{r}), \nabla \rho_n(\mathbf{r}), \tau_n(\mathbf{r}), \mathbf{J}_n(\mathbf{r}), \rho_p(\mathbf{r}), \nabla \rho_p(\mathbf{r}), \tau_p(\mathbf{r}), \mathbf{J}_p(\mathbf{r}) \right] \\ & + \mathcal{E}_{\text{Coul}} \left[ \rho_p(\mathbf{r}) \right] + \mathcal{E}_{\text{pair}} \left[ \rho_n(\mathbf{r}), \tilde{\rho}_n(\mathbf{r}), \rho_p(\mathbf{r}), \tilde{\rho}_p(\mathbf{r}) \right] \quad . \end{aligned} \quad (\text{A2})$$

The first term here, the energy density for the Skyrme force of this paper, is given by

$$\begin{aligned}
\mathcal{E}_{\text{Sky}} = & \sum_{q=n,p} \frac{\hbar^2}{2M_q} \tau_q + \frac{1}{2} t_0 \left[ \left(1 + \frac{1}{2} x_0\right) \rho^2 - \left(\frac{1}{2} + x_0\right) \sum_{q=n,p} \rho_q^2 \right] \\
& + \frac{1}{4} t_1 \left[ \left(1 + \frac{1}{2} x_1\right) \left(\rho\tau + \frac{3}{4}(\nabla\rho)^2\right) - \left(\frac{1}{2} + x_1\right) \sum_{q=n,p} \left(\rho_q\tau_q + \frac{3}{4}(\nabla\rho_q)^2\right) \right] \\
& + \frac{1}{4} t_2 \left[ \left(1 + \frac{1}{2} x_2\right) \left(\rho\tau - \frac{1}{4}(\nabla\rho)^2\right) + \left(\frac{1}{2} + x_2\right) \sum_{q=n,p} \left(\rho_q\tau_q - \frac{1}{4}(\nabla\rho_q)^2\right) \right] \\
& + \frac{1}{12} t_3 \rho^\alpha \left[ \left(1 + \frac{1}{2} x_3\right) \rho^2 - \left(\frac{1}{2} + x_3\right) \sum_{q=n,p} \rho_q^2 \right] \\
& + \frac{1}{4} t_4 \left[ \left(1 + \frac{1}{2} x_4\right) \left(\rho\tau + \frac{3}{4}(\nabla\rho)^2\right) - \left(\frac{1}{2} + x_4\right) \sum_{q=n,p} \left(\rho_q\tau_q + \frac{3}{4}(\nabla\rho_q)^2\right) \right] \rho^\beta \\
& + \frac{\beta}{8} t_4 \left[ \left(1 + \frac{1}{2} x_4\right) \rho(\nabla\rho)^2 - \left(\frac{1}{2} + x_4\right) \nabla\rho \cdot \sum_{q=n,p} \rho_q \nabla\rho_q \right] \rho^{\beta-1} \\
& + \frac{1}{4} t_5 \left[ \left(1 + \frac{1}{2} x_5\right) \left(\rho\tau - \frac{1}{4}(\nabla\rho)^2\right) + \left(\frac{1}{2} + x_5\right) \sum_{q=n,p} \left(\rho_q\tau_q - \frac{1}{4}(\nabla\rho_q)^2\right) \right] \rho^\gamma \\
& - \frac{1}{16} (t_1 x_1 + t_2 x_2) J^2 + \frac{1}{16} (t_1 - t_2) \sum_{q=n,p} J_q^2 \\
& - \frac{1}{16} (t_4 x_4 \rho^\beta + t_5 x_5 \rho^\gamma) J^2 + \frac{1}{16} (t_4 \rho^\beta - t_5 \rho^\gamma) \sum_{q=n,p} J_q^2 \\
& + \frac{1}{2} W_0 \left( \mathbf{J} \cdot \nabla\rho + \sum_{q=n,p} \mathbf{J}_q \cdot \nabla\rho_q \right). \tag{A3}
\end{aligned}$$

It will be seen that the  $t_5$  term has the same form as the  $t_2$  term, multiplied by the  $\rho^\gamma$  factor. No such simple relation between the  $t_4$  and  $t_1$  terms is apparent, because we have eliminated terms containing a Laplacian, through integration by parts over the entire system (this accounts for the terms linear in  $\beta$ ).

The second term in Eq. (A2) is the Coulomb energy density, which, since we are neglecting Coulomb exchange (see Section IV), is given simply by

$$\mathcal{E}_{\text{Coul}} = \frac{1}{2} e \rho_{\text{ch}} V^{\text{Coul}}, \tag{A4}$$

in which  $e\rho_{\text{ch}}$  is the charge density associated with protons (this differs from  $e\rho_p$  because we are taking account of the finite size of the proton [24]), and  $V^{\text{Coul}}$  is the electrostatic

potential, given by

$$V^{\text{Coul}}(\mathbf{r}) = e \int d^3\mathbf{r}' \frac{\rho_{\text{ch}}(\mathbf{r}')}{|\mathbf{r} - \mathbf{r}'|}. \quad (\text{A5})$$

The last term in Eq. (A2) is the pairing-energy density, discussed fully in Refs. [1, 24].

*Self-consistent s.p. fields.* In coordinate-space (assuming time-reversal invariance), the HFB equations read

$$\sum_{\sigma'=\pm 1} \begin{pmatrix} h'_q(\mathbf{r})_{\sigma\sigma'} - \lambda_q \delta_{\sigma\sigma'} & \Delta_q(\mathbf{r})\delta_{\sigma\sigma'} \\ \Delta_q(\mathbf{r})\delta_{\sigma\sigma'} & -h'_q(\mathbf{r})_{\sigma\sigma'} + \lambda_q \delta_{\sigma\sigma'} \end{pmatrix} \begin{pmatrix} \psi_{1i}^{(q)}(\mathbf{r}, \sigma') \\ \psi_{2i}^{(q)}(\mathbf{r}, \sigma') \end{pmatrix} = E_i \begin{pmatrix} \psi_{1i}^{(q)}(\mathbf{r}, \sigma) \\ \psi_{2i}^{(q)}(\mathbf{r}, \sigma) \end{pmatrix}, \quad (\text{A6})$$

where the s.p. Hamiltonian  $h'_q(\mathbf{r})_{\sigma\sigma'}$  and pairing field  $\Delta_q(\mathbf{r})$  are given by

$$h'_q(\mathbf{r})_{\sigma'\sigma} \equiv -\nabla \cdot \frac{\hbar^2}{2M_q^*(\mathbf{r})} \nabla \delta_{\sigma\sigma'} + U_q(\mathbf{r})\delta_{\sigma\sigma'} - \mathbf{i}\mathbf{W}_q(\mathbf{r}) \cdot \nabla \times \boldsymbol{\sigma}_{\sigma'\sigma} \quad (\text{A7})$$

and

$$\Delta_q(\mathbf{r}) = \frac{\partial \mathcal{E}_{\text{HFB}}(\mathbf{r})}{\partial \tilde{\rho}_q(\mathbf{r})} = \frac{1}{2} v^{\pi q} [\rho_n(\mathbf{r}), \rho_p(\mathbf{r})] \tilde{\rho}_q(\mathbf{r}). \quad (\text{A8})$$

The s.p. fields appearing in Eq. (A7) are defined by

$$\frac{\hbar^2}{2M_q^*(\mathbf{r})} = \frac{\partial \mathcal{E}_{\text{HFB}}(\mathbf{r})}{\partial \tau_q(\mathbf{r})}, \quad U_q(\mathbf{r}) = \frac{\partial \mathcal{E}_{\text{HFB}}(\mathbf{r})}{\partial \rho_q(\mathbf{r})} - \nabla \cdot \frac{\partial \mathcal{E}_{\text{HFB}}(\mathbf{r})}{\partial (\nabla \rho_q(\mathbf{r}))}, \quad \mathbf{W}_q(\mathbf{r}) = \frac{\partial \mathcal{E}_{\text{HFB}}(\mathbf{r})}{\partial \mathbf{J}_q(\mathbf{r})}. \quad (\text{A9})$$

From Eq. (A3), we find

$$\begin{aligned} \frac{\hbar^2}{2M_q^*} &= \frac{\hbar^2}{2M_q} + \frac{1}{4} t_1 \left[ \left(1 + \frac{1}{2} x_1\right) \rho - \left(\frac{1}{2} + x_1\right) \rho_q \right] + \frac{1}{4} t_2 \left[ \left(1 + \frac{1}{2} x_2\right) \rho + \left(\frac{1}{2} + x_2\right) \rho_q \right] \\ &+ \frac{1}{4} t_4 \left[ \left(1 + \frac{1}{2} x_4\right) \rho - \left(\frac{1}{2} + x_4\right) \rho_q \right] \rho^\beta + \frac{1}{4} t_5 \left[ \left(1 + \frac{1}{2} x_5\right) \rho + \left(\frac{1}{2} + x_5\right) \rho_q \right] \rho^\gamma, \end{aligned} \quad (\text{A10})$$

$$\begin{aligned}
U_q = & t_0 \left[ \left(1 + \frac{1}{2}x_0\right) \rho - \left(\frac{1}{2} + x_0\right) \rho_q \right] \\
& + \frac{1}{4}t_1 \left[ \left(1 + \frac{1}{2}x_1\right) \left(\tau - \frac{3}{2}\nabla^2\rho\right) - \left(\frac{1}{2} + x_1\right) \left(\tau_q - \frac{3}{2}\nabla^2\rho_q\right) \right] \\
& + \frac{1}{4}t_2 \left[ \left(1 + \frac{1}{2}x_2\right) \left(\tau + \frac{1}{2}\nabla^2\rho\right) + \left(\frac{1}{2} + x_2\right) \left(\tau_q + \frac{1}{2}\nabla^2\rho_q\right) \right] \\
& + \frac{1}{12}t_3 \left[ \left(1 + \frac{1}{2}x_3\right) (2 + \alpha)\rho^{\alpha+1} - \left(\frac{1}{2} + x_3\right) \left(2\rho^\alpha\rho_q + \alpha\rho^{\alpha-1} \sum_{q'=n,p} \rho_{q'}^2\right) \right] \\
& + \frac{1}{8}t_4 \left[ \left(1 + \frac{1}{2}x_4\right) \rho^{\beta-1} \left\{ 2(1 + \beta)\rho\tau - (2\beta + 3)\left(\frac{1}{2}\beta(\nabla\rho)^2 + \rho\nabla^2\rho\right) \right\} \right. \\
& + \left. \left(\frac{1}{2} + x_4\right) \rho^{\beta-2} \left\{ 3\beta\rho\nabla\rho \cdot \nabla\rho_q + 3\rho^2\nabla^2\rho_q - 2\rho^2\tau_q \right. \right. \\
& + \left. \left. \beta(\beta - 1)\rho_q(\nabla\rho)^2 + \beta\rho\rho_q\nabla^2\rho - \frac{1}{2}\beta\rho \sum_{q'=n,p} \left[ (\nabla\rho_{q'})^2 + 4\rho_{q'}\tau_{q'} - 2\rho_{q'}\nabla^2\rho_{q'} \right] \right\} \right] \\
& + \frac{1}{4}t_5 \left[ \left(1 + \frac{1}{2}x_5\right) \left\{ (1 + \gamma)\rho\tau + \frac{1}{4}\gamma(\nabla\rho)^2 + \frac{1}{2}\rho\nabla^2\rho \right\} \right. \\
& + \left. \left(\frac{1}{2} + x_5\right) \left\{ \rho\tau_q + \frac{1}{2}\rho\nabla^2\rho_q + \gamma \sum_{q'=n,p} \left\{ \rho_{q'}\tau_{q'} - \frac{1}{4}(\nabla\rho_{q'})^2 \right\} + \frac{1}{2}\gamma\nabla\rho \cdot \nabla\rho_q \right\} \right] \rho^{\gamma-1} \\
& - \frac{1}{16}(t_4x_4\beta\rho^{\beta-1} + t_5x_5\gamma\rho^{\gamma-1})J^2 + \frac{1}{16}(t_4\beta\rho^{\beta-1} - t_5\gamma\rho^{\gamma-1}) \sum_{q'=n,p} J_{q'}^2 \\
& - \frac{1}{2}W_0(\nabla \cdot \mathbf{J} + \nabla \cdot \mathbf{J}_q) + \delta_{q,p}V^{\text{Coul}} + \frac{1}{4} \sum_{q'=n,p} \frac{\partial v^{\pi q'}}{\partial \rho_q} \tilde{\rho}_{q'}^2 \tag{A11}
\end{aligned}$$

and

$$\begin{aligned}
\mathbf{W}_q = & \frac{1}{2}W_0\nabla(\rho + \rho_q) - \frac{1}{8}(t_1x_1 + t_2x_2)\mathbf{J} + \frac{1}{8}(t_1 - t_2)\mathbf{J}_q \\
& - \frac{1}{8}(t_4x_4\rho^\beta + t_5x_5\rho^\gamma)\mathbf{J} + \frac{1}{8}(t_4\rho^\beta - t_5\rho^\gamma)\mathbf{J}_q. \tag{A12}
\end{aligned}$$

The Coulomb field  $V^{\text{Coul}}(\mathbf{r})$  is given by Eq. (A5).

*Unpolarized homogeneous nuclear matter.* For the energy per nucleon of infinite nuclear

matter of density  $\rho$  and asymmetry  $\eta$  (defined by  $\eta = (\rho_n - \rho_p)/\rho$ ), Eq. (A3) reduces to

$$\begin{aligned}
e = & \frac{3\hbar^2}{20} k_F^2 \left\{ \frac{1}{M_n} (1 + \eta)^{5/3} + \frac{1}{M_p} (1 - \eta)^{5/3} \right\} \\
& + \frac{1}{8} t_0 \left[ 3 - (2x_0 + 1)\eta^2 \right] \rho \\
& + \frac{3}{40} t_1 \left[ (2 + x_1)F_{5/3}(\eta) - \left(\frac{1}{2} + x_1\right)F_{8/3}(\eta) \right] \rho k_F^2 \\
& + \frac{3}{40} t_2 \left[ (2 + x_2)F_{5/3}(\eta) + \left(\frac{1}{2} + x_2\right)F_{8/3}(\eta) \right] \rho k_F^2 \\
& + \frac{1}{48} t_3 \left[ 3 - (1 + 2x_3)\eta^2 \right] \rho^{\alpha+1} \\
& + \frac{3}{40} t_4 \left[ (2 + x_4)F_{5/3}(\eta) - \left(\frac{1}{2} + x_4\right)F_{8/3}(\eta) \right] \rho^{\beta+1} k_F^2 \\
& + \frac{3}{40} t_5 \left[ (2 + x_5)F_{5/3}(\eta) + \left(\frac{1}{2} + x_5\right)F_{8/3}(\eta) \right] \rho^{\gamma+1} k_F^2 \quad ,
\end{aligned} \tag{A13}$$

where

$$k_F = \left( \frac{3\pi^2 \rho}{2} \right)^{1/3} \tag{A14}$$

and

$$F_x(\eta) = \frac{1}{2} \left[ (1 + \eta)^x + (1 - \eta)^x \right] \quad . \tag{A15}$$

For SNM ( $\eta = 0$ ) Eq. (A13) reduces to

$$\begin{aligned}
e(\eta = 0) = & \frac{3\hbar^2}{10M} k_F^2 + \frac{3}{8} t_0 \rho + \frac{3}{80} \left[ 3t_1 + t_2(5 + 4x_2) \right] \rho k_F^2 + \frac{1}{16} t_3 \rho^{\alpha+1} \\
& + \frac{9}{80} t_4 \rho^{\beta+1} k_F^2 + \frac{3}{80} t_5 (5 + 4x_5) \rho^{\gamma+1} k_F^2 \quad ,
\end{aligned} \tag{A16}$$

where

$$\frac{2}{M} = \frac{1}{M_n} + \frac{1}{M_p} \quad . \tag{A17}$$

From Eq. (A17) we have

$$\begin{aligned}
k_F^2 \frac{\partial^2 e}{\partial k_F^2} \Big|_{\eta=0} &= \frac{3\hbar^2}{5M} k_F^2 + \frac{9}{4} t_0 \rho + \frac{3}{4} \left[ 3t_1 + t_2(5 + 4x_2) \right] \rho k_F^2 \\
&+ \frac{3}{16} t_3 (\alpha + 1) (3\alpha + 2) \rho^{\alpha+1} \\
&+ \frac{9}{80} t_4 (3\beta + 5) (3\beta + 4) \rho^{\beta+1} k_F^2 \\
&+ \frac{3}{80} t_5 (5 + 4x_5) (3\gamma + 5) (3\gamma + 4) \rho^{\gamma+1} k_F^2 \quad .
\end{aligned} \tag{A18}$$

Evaluating this at  $\rho = \rho_0$  and introducing  $k_{F0} = (3\pi^2 \rho_0 / 2)^{1/3}$  defines the usual incompressibility

$$K_v = k_{F0}^2 \frac{\partial^2 e}{\partial k_F^2} \Big|_{\eta=0, \rho=\rho_0} = 9\rho_0^2 \frac{\partial^2 e}{\partial \rho_0^2} \Big|_{\eta=0, \rho=\rho_0} \quad , \tag{A19}$$

the two forms being equivalent only because at  $\rho = \rho_0$  we have

$$\frac{\partial e}{\partial \rho} \Big|_{\eta=0, \rho=\rho_0} = 0 \quad . \tag{A20}$$

Expanding  $(1 \pm \eta)^x$  up to  $\eta^2$  allows us to rewrite Eq. (A13) as

$$e = e(\eta = 0) + \frac{\hbar^2}{4} k_F^2 \left( \frac{1}{M_n} - \frac{1}{M_p} \right) \eta + e_{sym} \eta^2 + O(\eta^4) \quad , \tag{A21}$$

where we have introduced the symmetry energy

$$\begin{aligned}
e_{sym}(\rho) &= \frac{\hbar^2}{6M} k_F^2 - \frac{1}{8} t_0 (2x_0 + 1) \rho + \frac{1}{24} \left[ -3t_1 x_1 + t_2 (4 + 5x_2) \right] \rho k_F^2 \\
&- \frac{1}{48} t_3 (1 + 2x_3) \rho^{\alpha+1} - \frac{1}{8} t_4 x_4 \rho^{\beta+1} k_F^2 + \frac{1}{24} t_5 (4 + 5x_5) \rho^{\gamma+1} k_F^2 \quad (A22)
\end{aligned}$$

(note the breaking of charge symmetry implied by the neutron-proton mass difference; this is explicitly included in the finite-nucleus calculations). The usual symmetry coefficient [28] is then given by

$$J = e_{sym}(\rho_0) \quad . \tag{A23}$$

For the density-symmetry coefficient [28] defined by

$$L = k_{F0} \frac{de_{sym}}{dk_F} \Big|_{\rho=\rho_0} = 3\rho_0 \frac{de_{sym}}{d\rho} \Big|_{\rho=\rho_0} \quad , \tag{A24}$$

it follows from Eq. (A22) that

$$\begin{aligned}
L = & \frac{\hbar^2}{3M} k_{F0}^2 - \frac{3}{8} t_0 (2x_0 + 1) \rho_0 + \frac{5}{24} \left[ -3t_1 x_1 + t_2 (4 + 5x_2) \right] \rho_0 k_{F0}^2 \\
& - \frac{\alpha + 1}{16} t_3 (1 + 2x_3) \rho_0^{\alpha+1} - \frac{5 + 3\beta}{8} t_4 x_4 \rho_0^{\beta+1} k_{F0}^2 \\
& + \frac{5 + 3\gamma}{24} t_5 (4 + 5x_5) \rho_0^{\gamma+1} k_{F0}^2 \quad . \quad (A25)
\end{aligned}$$

Setting  $\eta = 1$  in Eq. (A13) gives us for the energy per nucleon in unpolarized NeuM

$$\begin{aligned}
e = & \frac{3\hbar^2}{10M_n} k_{Fn}^2 + \frac{1}{4} t_0 (1 - x_0) \rho + \frac{3}{40} t_1 (1 - x_1) \rho k_{Fn}^2 + \frac{9}{40} t_2 (1 + x_2) \rho k_{Fn}^2 \\
& + \frac{1}{24} t_3 (1 - x_3) \rho^{\alpha+1} + \frac{3}{40} t_4 (1 - x_4) \rho^{\beta+1} k_{Fn}^2 + \frac{9}{40} t_5 (1 + x_5) \rho^{\gamma+1} k_{Fn}^2 \quad , \quad (A26)
\end{aligned}$$

where

$$k_{Fn} = (3\pi^2 \rho)^{1/3} \quad (A27)$$

(Eq. (A26) cannot be derived from Eqs. (A21) and (A22)).

Note that the terms in  $t_4$  and  $t_5$  will not contribute to any of the foregoing expressions for homogeneous unpolarized matter if the conditions (8), (10) and (11) are satisfied.

#### *Polarized nuclear matter*

In general the Skyrme energy density can be decomposed into a time-even part  $\mathcal{E}_{\text{Sky}}^{\text{even}}$  given by Eq. (A3) and a time-odd part  $\mathcal{E}_{\text{Sky}}^{\text{odd}}$  which is non-zero only when time-reversal invariance is not satisfied. In polarized homogeneous nuclear matter these two parts take the form

$$\mathcal{E}_{\text{Sky}}^{\text{even}} = \sum_{q=n,p} \frac{\hbar^2}{2M_q} \tau_q + C_0^\rho \rho^2 + C_1^\rho (\rho_n - \rho_p)^2 + C_0^\tau \rho \tau + C_1^\tau (\rho_n - \rho_p) (\tau_n - \tau_p) \quad , \quad (A28)$$

and

$$\mathcal{E}_{\text{Sky}}^{\text{odd}} = C_0^s \mathbf{s}^2 + C_1^s (\mathbf{s}_n - \mathbf{s}_p)^2 + C_0^T \mathbf{s} \cdot \mathbf{T} + C_1^T (\mathbf{s}_n - \mathbf{s}_p) \cdot (\mathbf{T}_n - \mathbf{T}_p) \quad (A29)$$

where  $\mathbf{s}_q$  and  $\mathbf{T}_q$  are the spin density and kinetic spin density respectively (for a precise definition, see, for example, Bender *et al.* [19]), and  $\mathbf{s} = \mathbf{s}_n + \mathbf{s}_p$ ,  $\mathbf{T} = \mathbf{T}_n + \mathbf{T}_p$ .

The expressions for the coefficients appearing in Eqs. (A28) and (A29) in the case of the conventional Skyrme force (1) can be found, for example, in Appendix B of Ref. [19]. The coefficients  $C_0^\rho$ ,  $C_1^\rho$ ,  $C_0^s$  and  $C_1^s$  depend only on the  $t_0$  and  $t_3$  terms of the Skyrme force (1) and therefore remain unchanged when the new terms of Eq. (2) are included. This is not the

case for the other coefficients. However  $C_0^\tau$  and  $C_1^\tau$  can be readily obtained by comparing Eqs. (A28) and (A3). The expressions for the remaining coefficients  $C_0^T$  and  $C_1^T$  can also be obtained from Eq. (A3) using the gauge invariance of the Skyrme force [33, 34]:  $-C_0^T$  and  $-C_1^T$  coincide with the coefficients in front of the terms proportional to  $J^2$  and  $(\mathbf{J}_n - \mathbf{J}_p)^2$  in Eq. (A3). The various coefficients are thus given by

$$C_0^\rho = \frac{3}{8}t_0 + \frac{3}{48}t_3\rho^\alpha \quad (\text{A30a})$$

$$C_1^\rho = -\frac{1}{4}t_0 \left( \frac{1}{2} + x_0 \right) - \frac{1}{24}t_3(1 + x_3)\rho^\alpha \quad (\text{A30b})$$

$$C_0^s = -\frac{1}{4}t_0 \left( \frac{1}{2} - x_0 \right) - \frac{1}{24}t_3 \left( \frac{1}{2} - x_3 \right) \rho^\alpha \quad (\text{A30c})$$

$$C_1^s = -\frac{1}{8}t_0 - \frac{1}{48}t_3\rho^\alpha \quad (\text{A30d})$$

$$C_0^\tau = \frac{3}{16}t_1 + \frac{1}{4}t_2 \left( \frac{5}{4} + x_2 \right) + \frac{3}{16}t_4\rho^\beta + \frac{1}{4}t_5 \left( \frac{5}{4} + x_5 \right) \rho^\gamma \quad (\text{A30e})$$

$$C_1^\tau = -\frac{1}{8}t_1 \left( \frac{1}{2} + x_1 \right) + \frac{1}{8}t_2 \left( \frac{1}{2} + x_2 \right) - \frac{1}{8}t_4\rho^\beta \left( \frac{1}{2} + x_4 \right) + \frac{1}{8}t_5\rho^\gamma \left( \frac{1}{2} + x_5 \right) \quad (\text{A30f})$$

$$C_0^T = -\frac{1}{8} \left[ t_1 \left( \frac{1}{2} - x_1 \right) - t_2 \left( \frac{1}{2} + x_2 \right) + t_4\rho^\beta \left( \frac{1}{2} - x_4 \right) - t_5\rho^\gamma \left( \frac{1}{2} + x_5 \right) \right] \quad (\text{A30g})$$

$$C_1^T = -\frac{1}{16}(t_1 - t_2) - \frac{1}{16}(t_4\rho^\beta - t_5\rho^\gamma). \quad (\text{A30h})$$

Under the constraints (8), (9) and (10), the new terms in the Skyrme force do not affect the coefficients  $C_0^\tau$  and  $C_1^\tau$ . In the particular case of model HFB-18 for which  $t_4 = t_5$ , the coefficient  $C_1^T$  is also unchanged, so that only  $C_0^T$  changes.

It can thus be seen that the expressions of the above  $C$ -coefficients given in Ref.[19] can be extended to the generalized Skyrme force (5) simply by making the following substitutions:

$$t_1 \rightarrow t_1 + t_4 \rho^\beta \quad , \quad (\text{A31a})$$

$$t_1 x_1 \rightarrow t_1 x_1 + t_4 x_4 \rho^\beta \quad , \quad (\text{A31b})$$

$$t_2 \rightarrow t_2 + t_5 \rho^\gamma \quad , \quad (\text{A31c})$$

$$t_2 x_2 \rightarrow t_2 x_2 + t_5 x_5 \rho^\gamma \quad . \quad (\text{A31d})$$

With this simple rule, the expression for the energy per nucleon of asymmetric polarized homogeneous nuclear matter can be easily obtained from Eq. (C.14) of Ref. [19].

#### *Landau parameters*

The dimensionless Landau parameters for symmetric nuclear matter corresponding to the generalized Skyrme force (5) are given in terms of the C-coefficients of Eqs. (A30a) - (A30h) by

$$F_0 = N_0 \left[ 2C_0^\rho + 2C_0^\tau k_F^2 + 4\rho \frac{dC_0^\rho}{d\rho} + \rho^2 \frac{d^2 C_0^\rho}{d\rho^2} + \rho\tau \frac{d^2 C_0^\tau}{d\rho^2} + \frac{dC_0^\tau}{d\rho} (2\tau + 2\rho k_F^2) \right] \quad (\text{A32a})$$

$$F'_0 = N_0 \left[ 2C_1^\rho + 2C_1^\tau k_F^2 \right] \quad (\text{A32b})$$

$$F_1 = -2N_0 C_0^\tau k_F^2 \quad (\text{A32c})$$

$$F'_1 = -2N_0 C_1^\tau k_F^2 \quad (\text{A32d})$$

$$G_0 = N_0 \left[ 2C_0^s + 2C_0^T k_F^2 \right] \quad (\text{A32e})$$

$$G'_0 = N_0 \left[ 2C_1^s + 2C_1^T k_F^2 \right] \quad (\text{A32f})$$

$$G_1 = -2N_0 C_0^T k_F^2 \quad (\text{A32g})$$

$$G'_1 = -2N_0 C_1^T k_F^2 \quad (\text{A32h})$$

where  $N_0$  is the density of s.p. states at the Fermi level

$$N_0 = \frac{2M_s^* k_F}{\hbar^2 \pi^2}. \quad (\text{A33})$$

For the conventional Skyrme force (1), the above expressions reduce to those given in Appendix D of Ref.[19]. Since with BSk18  $C_0^T$  is the only C-coefficient that is modified by the  $t_4$  and  $t_5$  terms it follows that they affect only the Landau parameters  $G_0$  and  $G_1$ .

- 
- [1] S. Goriely, N. Chamel, and J. M. Pearson, Phys. Rev. Lett. **102**, 152503 (2009).
  - [2] S. Goriely, M. Samyn, J. M. Pearson, and M. Onsi, Nucl. Phys. **A750**, 425 (2005).
  - [3] B. Friedman and V. R. Pandharipande, Nucl. Phys. **A361**, 502 (1981).
  - [4] A. Akmal, V. R. Pandharipande, and D. G. Ravenhall, Phys. Rev. C **58**, 1804 (1998).
  - [5] Z. Xiao, B.-A. Li, L.-W. Chen, G.-C. Yong, and M. Zhang, Phys. Rev. Lett. **102**, 062502 (2009).
  - [6] M. Onsi, A. K. Dutta, H. Chatri, S. Goriely, N. Chamel, and J. M. Pearson, Phys. Rev. C **77** 065805, (2008).
  - [7] A. Vidaurre, J. Navarro, and J. Bernabéu, Astron. Astrophys. **135**, 361 (1984).
  - [8] M. Kutschera and W. Wójcik, Phys. Lett. **B325**, 271 (1994).
  - [9] J. Margueron, J. Navarro, and N.V. Giai, Phys. Rev. C **66**, 014303 (2002).
  - [10] S. Fantoni, A. Sarsa, and K. E. Schmidt, Phys. Rev. Lett. **87**, 181101 (2001).
  - [11] I. Bombaci, A. Polls, A. Ramos, A. Rios, and I. Vidaña, Phys. Lett. **B 632**, 638 (2006).
  - [12] F. Sammarruca and P. G. Krastev, Phys. Rev. C **75**, 034315 (2007).
  - [13] G. H. Bordbar and M. Bigdeli, Phys. Rev. C **78**, 054315 (2008).
  - [14] I. Vidaña and I. Bombaci, Phys. Rev. C **66**, 045801 (2002).
  - [15] G. H. Bordbar and M. Bigdeli, Phys. Rev. C **77**, 015805 (2008).
  - [16] J. Margueron and H. Sagawa, J. Phys. G: Nucl.Part.Phys. **36**, 125102 (2009).
  - [17] J. Margueron, S. Goriely, M. Grasso, G. Colo, and H. Sagawa, J. Phys. G: Nucl.Part.Phys. **36**, 125103 (2009).
  - [18] E. Chabanat, P. Bonche, P. Haensel, J. Meyer, and R. Schaeffer, Nucl. Phys. **A635**, 231 (1998); Nucl. Phys. **A643**, 441 (1998).

- [19] M. Bender, J. Dobaczewski, J. Engel, and W. Nazarewicz, *Phys. Rev. C* **65**, 054322 (2002).
- [20] A. Weiss, W. Hillebrandt, H.-C. Thomas, and H. Ritter, *Cox and Giuli's Principles of Stellar Structure*, extended second edition. Cambridge Scientific Publishers (2004).
- [21] M.V. Stoitsov, J. Dobaczewski, W. Nazarewicz, S. Pittel, and D.J. Dean, *Phys. Rev. C* **68**, 054312 (2003).
- [22] L .G. Cao, U. Lombardo, and P. Schuck, *Phys. Rev. C* **74**, 064301 (2006).
- [23] S. Goriely, M. Samyn, P.-H. Heenen, J. M. Pearson, and F. Tondeur, *Phys. Rev. C* **66**, 024326 (2002).
- [24] N. Chamel, S. Goriely, and J. M. Pearson, *Nucl. Phys.* **A812**, 72 (2008).
- [25] S. Goriely and J. M. Pearson, *Phys. Rev. C* **77**, 031301(R) (2008).
- [26] G. Audi, A.H. Wapstra, and C. Thibault, *Nucl. Phys.* **A729**, 337 (2003).
- [27] M. Farine, J. M. Pearson, and F. Tondeur, *Nucl. Phys.* **A696**, 396 (2001).
- [28] W. D. Myers and W. J. Swiatecki, *Ann. Phys. (N. Y.)* **55**, 395 (1969).
- [29] J. Duffo and A. P. Zuker, *Phys. Rev. C* **52**, R23 (1995).
- [30] M. Brack, C. Guet, and H.-B. Håkansson, *Physics Reports* **123**, 275 (1985).
- [31] S. Krewald, V. Klemt, J. Speth, and A. Faessler, *Nucl. Phys.* **A281**, 166 (1977).
- [32] I. Angeli, *At. Data and Nucl. Data Tables* **87**, 185 (2004).
- [33] Y. M. Engel, D. M. Brink, K. Goeke, S. J. Krieger, and D. Vautherin, *Nucl. Phys.* **A249**, 215 (1975).
- [34] J. Dobaczewski and J. Dudek, *Phys. Rev. C* **52**, 1827 (1995).

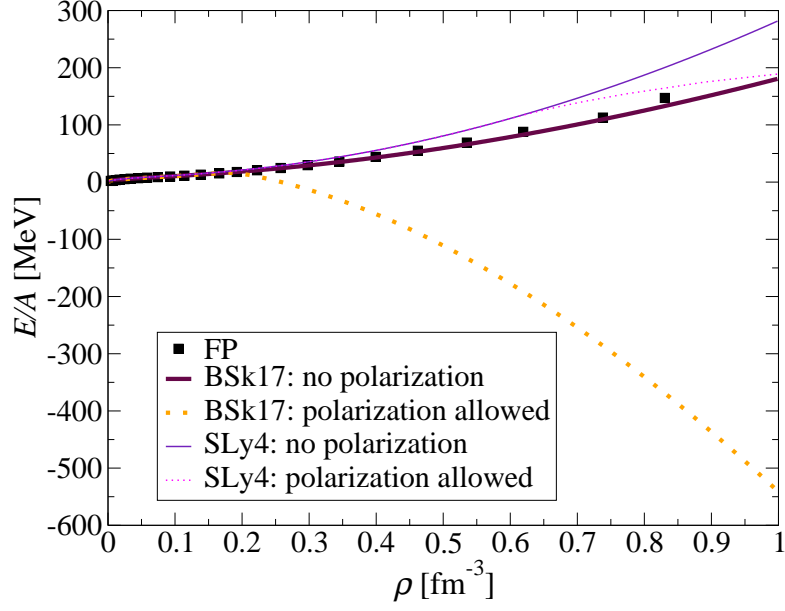


FIG. 1: (Color online) Energy per nucleon ( $T=0$ ) for pure neutron matter (NeuM) with forces BSk17 and SLy4. The squares are the results of the realistic calculations from Friedman and Pandharipande [3].

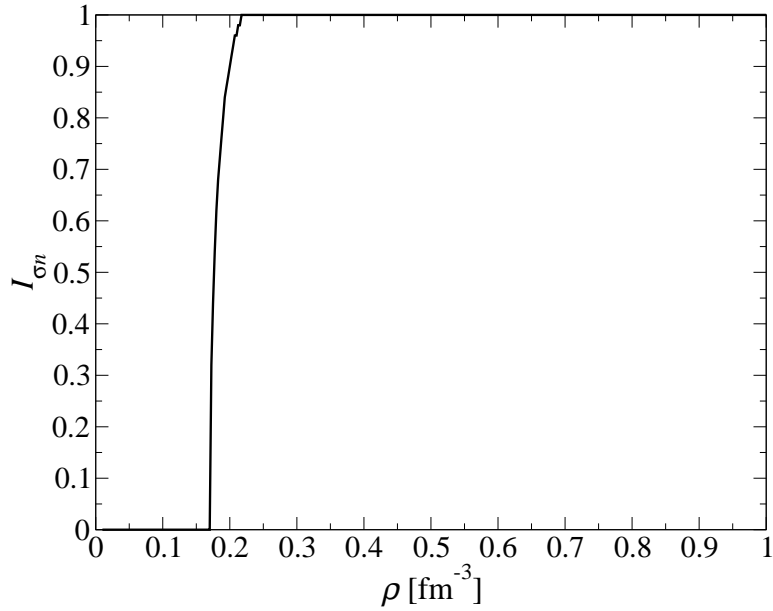


FIG. 2: Neutron polarization  $I_{\sigma n}$  for pure neutron matter (NeuM) with force BSk17.

TABLE I: Force BSk18: lines 1-16 show the Skyrme parameters, lines 17-21 the pairing parameters, and the last four lines the Wigner parameters (see text for further details). For convenience of comparison we also show model HFB-17 [1] (note that in the latter reference there were misprints in the pairing parameters  $f_q^\pm$ ).

	HFB-18	HFB-17
$t_0$ [MeV fm <sup>3</sup> ]	-1837.96	-1837.33
$t_1$ [MeV fm <sup>5</sup> ]	428.880	389.102
$t_2$ [MeV fm <sup>5</sup> ]	-3.23704	-3.17417
$t_3$ [MeV fm <sup>3+3<math>\alpha</math></sup> ]	11528.9	11523.8
$t_4$ [MeV fm <sup>5+3<math>\beta</math></sup> ]	-400.000	-
$t_5$ [MeV fm <sup>5+3<math>\gamma</math></sup> ]	-400.000	-
$x_0$	0.421290	0.411377
$x_1$	-0.907175	-0.832102
$x_2$	57.7185	49.4875
$x_3$	0.683926	0.654962
$x_4$	-2.00000	-
$x_5$	-2.00000	-
$W_0$ [MeV fm <sup>5</sup> ]	138.904	145.885
$\alpha$	0.3	0.3
$\beta$	1.0	-
$\gamma$	1.0	-
$f_n^+$	1.00	1.00
$f_n^-$	1.06	1.05
$f_p^+$	1.04	1.04
$f_p^-$	1.09	1.10
$\varepsilon_\Lambda$ [MeV]	16.0	16.0
$V_W$ [MeV]	-2.10	-2.00
$\lambda$	340	320
$V'_W$ [MeV]	0.74	0.86
$A_0$	28	28

TABLE II: Parameters of Eq.(14) for collective correction to model HFB-18.

$b$ (MeV)	0.8
$c$	10.0
$d$ (MeV)	3.0
$l$	16.0
$\beta_2^0$	0.1

TABLE III: Rms ( $\sigma$ ) and mean ( $\bar{\epsilon}$ ) deviations between data and predictions for model HFB-18; for convenience of comparison we also show model HFB-17 [1]. The first pair of lines refers to all the 2149 measured masses  $M$  that were fitted [26], the second pair to the masses  $M_{nr}$  of the subset of 185 neutron-rich nuclei with  $S_n \leq 5.0$  MeV, the third pair to the neutron separation energies  $S_n$  (1988 measured values), the fourth pair to beta-decay energies  $Q_\beta$  (1868 measured values) and the fifth pair to charge radii (782 measured values [32]). The last line shows the calculated neutron-skin thickness of  $^{208}\text{Pb}$  for these models.

	HFB-18	HFB-17
$\sigma(M)$ [MeV]	0.585	0.581
$\bar{\epsilon}(M)$ [MeV]	0.007	-0.019
$\sigma(M_{nr})$ [MeV]	0.758	0.729
$\bar{\epsilon}(M_{nr})$ [MeV]	0.172	0.119
$\sigma(S_n)$ [MeV]	0.487	0.506
$\bar{\epsilon}(S_n)$ [MeV]	-0.012	-0.010
$\sigma(Q_\beta)$ [MeV]	0.561	0.583
$\bar{\epsilon}(Q_\beta)$ [MeV]	0.025	0.022
$\sigma(R_c)$ [fm]	0.0274	0.0300
$\bar{\epsilon}(R_c)$ [fm]	0.0016	-0.0114
$\theta(^{208}\text{Pb})$ [fm]	0.15	0.15

TABLE IV: Parameters of infinite nuclear matter for force BSk18; for convenience of comparison we also show force BSk17 [1].

	BSk18	BSk17
$a_v$ [MeV]	-16.063	-16.054
$\rho_0$ [fm <sup>-3</sup> ]	0.1586	0.1586
$J$ [MeV]	30.0	30.0
$K_v$ [MeV]	241.8	241.7
$L$ [MeV]	36.21	36.28
$M_s^*/M$	0.80	0.80
$M_v^*/M$	0.79	0.78
$F_0$	-0.12	-0.12
$F'_0$	0.97	0.97
$F_1$	-0.60	-0.60
$F_1'$	0.032	0.068
$G_0$	-0.33	-0.69
$G'_0$	0.46	0.50
$G_1$	1.23	1.55
$G'_1$	0.50	0.45

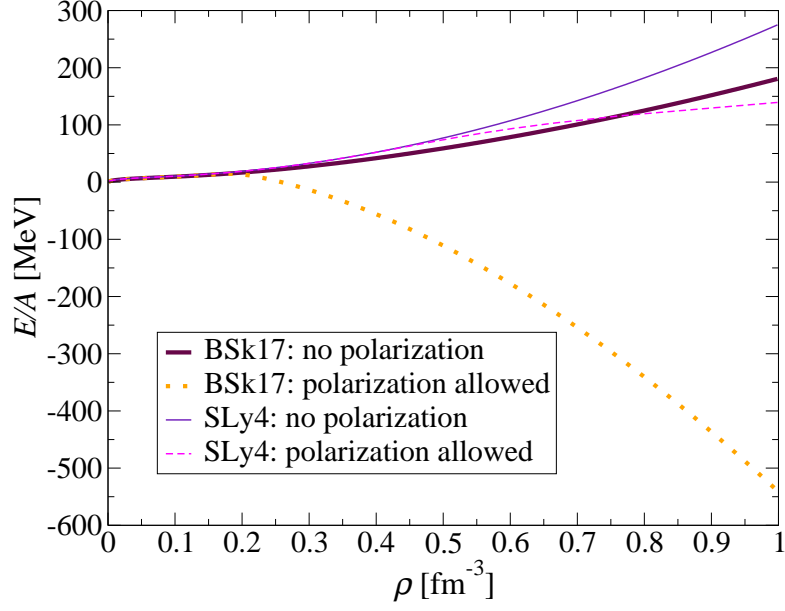


FIG. 3: (Color online) Energy per nucleon ( $T=0$ ) for neutron-star matter (N\*M) with forces BSk17 and SLy4.

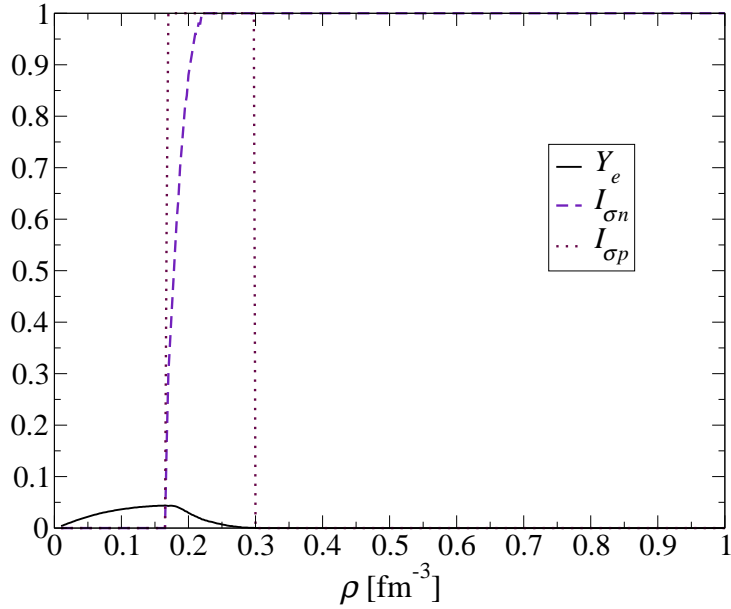


FIG. 4: (Color online) Proton fraction  $Y_e$ , neutron and proton polarizations  $I_{\sigma n}$  and  $I_{\sigma p}$ , respectively, for neutron-star matter (N\*M) with force BSk17.

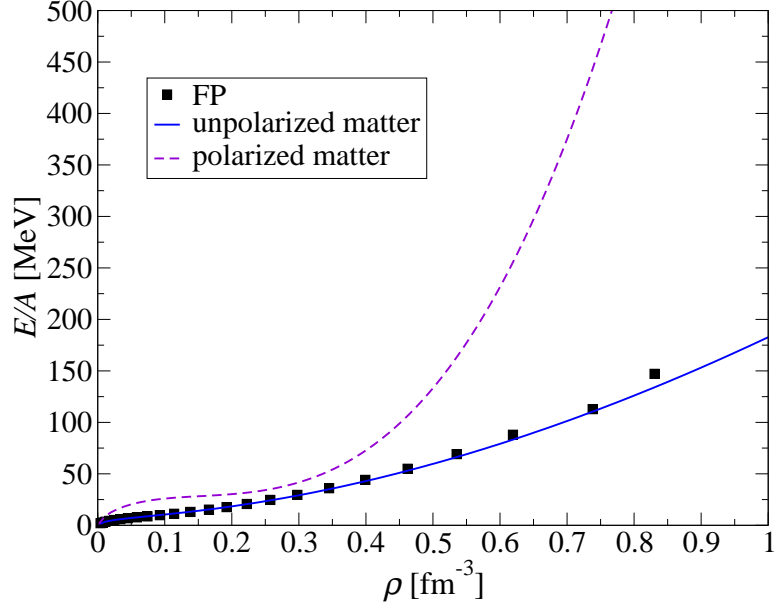


FIG. 5: (Color online) Energy per nucleon ( $T=0$ ) for pure neutron matter (NeuM), polarized and unpolarized, with force BSk18. The squares show the results of the realistic calculations of Friedman and Pandharipande [3].

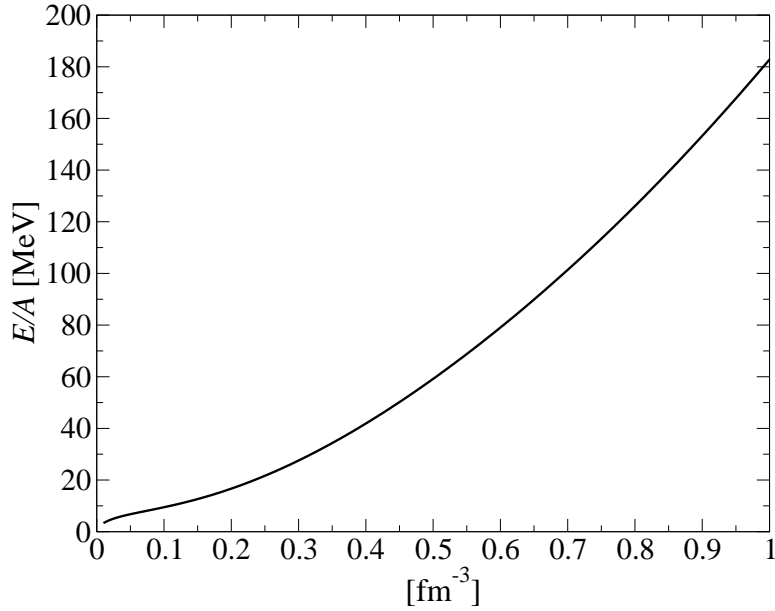


FIG. 6: Energy per nucleon ( $T=0$ ) for neutron-star matter (N\*M) with force BSk18. System stable against polarization in ground state.

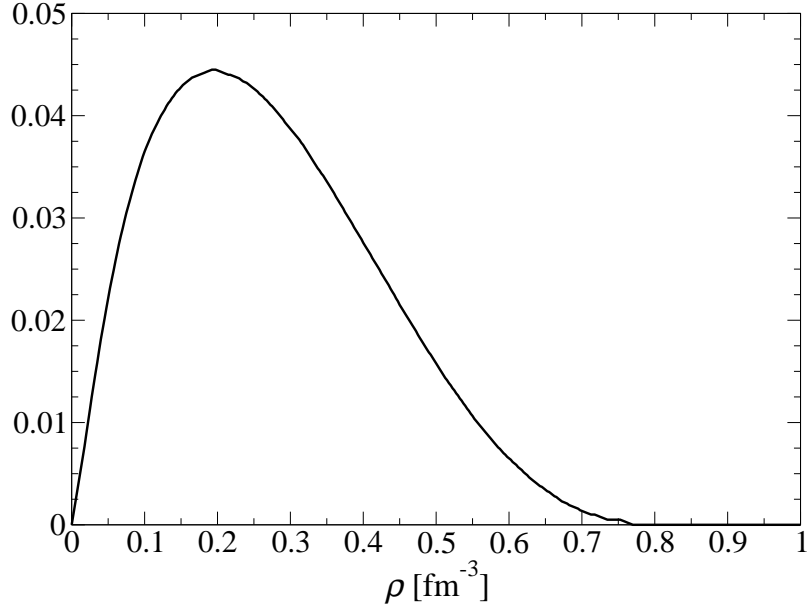


FIG. 7: Proton fraction  $Y_e$  for neutron-star matter (N\*M) with force BSk18.

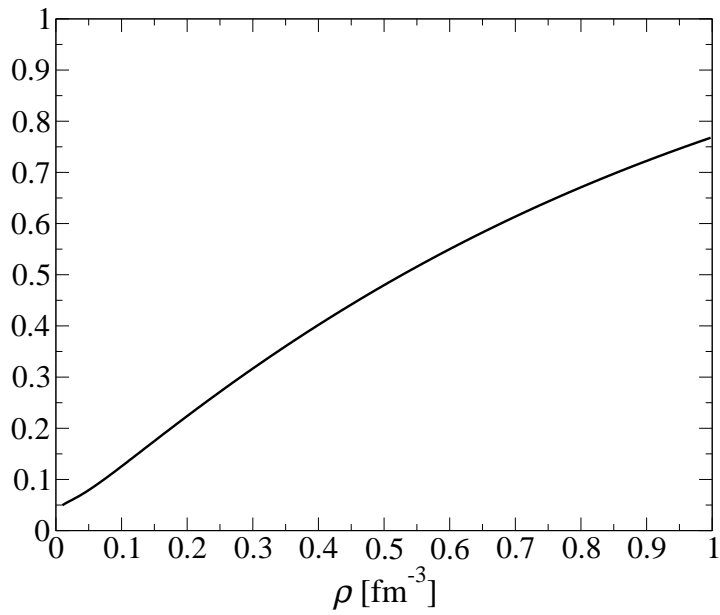


FIG. 8: Speed of sound  $v_s$  (in units of the light speed  $c$ ) for pure neutron-matter (NeuM) with force BSk18.

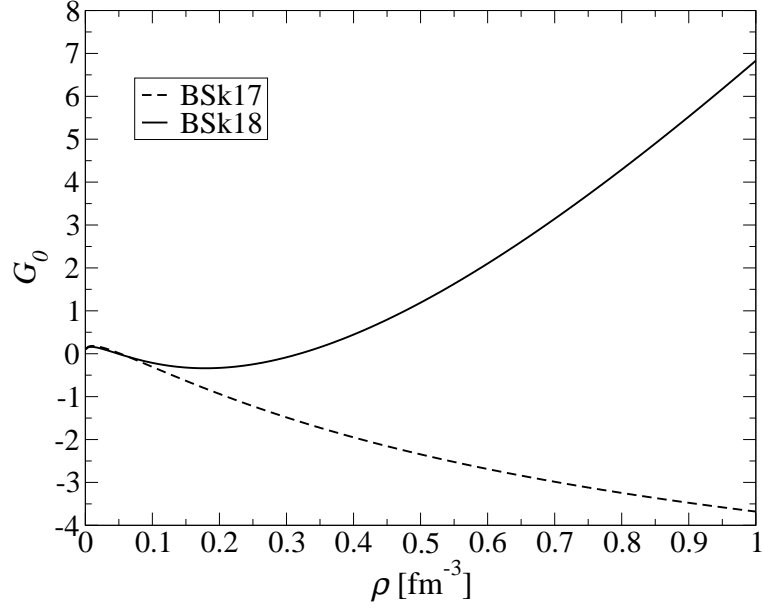


FIG. 9: Landau parameter  $G_0$  in symmetric nuclear matter for forces BSk17 (dashed line) and BSk18 (solid line).

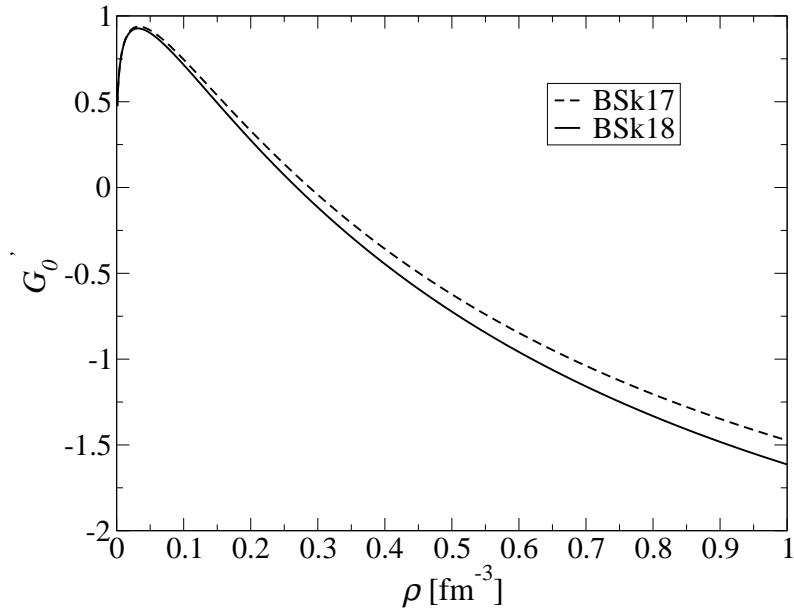


FIG. 10: Landau parameter  $G'_0$  in symmetric nuclear matter for forces BSk17 (dashed line) and BSk18 (solid line).